

# *In-Silico*-Assisted Derivatization of Triarylboranes for the Catalytic Reductive Functionalization of Amino Acids with H<sub>2</sub>

Yusei Hisata,<sup>1</sup> Takashi Washio,<sup>2</sup> Shinobu Takizawa,<sup>3</sup> Sensuke Ogoshi,<sup>1</sup> and Yoichi Hoshimoto\*<sup>1,4</sup>

[1] Department of Applied Chemistry, Faculty of Engineering, Osaka University, Suita, Osaka, 565-0871, Japan

[2] Department of Reasoning for Intelligence and Artificial Intelligence Research Center, SANKEN, Osaka University, Ibaraki, Osaka 567-0047, Japan

[3] Department of Synthetic Organic Chemistry and Artificial Intelligence Research Center, SANKEN, Osaka University, Ibaraki, Osaka 567-0047, Japan

[4] Center for Future Innovation (CFI), Division of Applied Chemistry, Faculty of Engineering, Osaka University, Suita, Osaka 565-0871, Japan

**KEYWORDS:** *Triarylboranes, Amino acids, Gaussian process regression, Machine learning, Reductive alkylation*

---

**ABSTRACT:** Cheminformatics-based machine learning (ML) has assisted in determining optimal reaction conditions, including catalyst structures, in the field of synthetic chemistry. However, such ML-focused strategies have remained largely unexplored in the context of catalytic molecular transformations using Lewis-acidic main-group elements, probably due to the absence of a candidate library and effective guidelines (parameters) for the prediction of the activity of main-group elements. Here, the construction of a triarylborane library and its application to an ML-assisted approach for the catalytic reductive alkylation of amino acids with aldehydes and H<sub>2</sub> is reported. The obtained results suggest that the deformation energy serves as a useful parameter for Gaussian process regression to construct adequate models for predicting the turnover frequencies of triarylboranes under the applied model reaction conditions, while Gaussian process regression based on the energy levels of the lowest unoccupied molecular orbitals (LUMOs) including the empty p-orbitals of boron tend to underestimate the turnover frequency. The optimal borane, i.e., B(2,3,5,6-Cl<sub>4</sub>-C<sub>6</sub>H)(2,6-F<sub>2</sub>-3,5-(CF<sub>3</sub>)<sub>2</sub>-C<sub>6</sub>H)<sub>2</sub>, effectively catalyzes the reductive functionalization of aniline-derived amino acids and C-terminal-protected peptides in the presence of 4-methyltetrahydropyran and H<sub>2</sub>, generating H<sub>2</sub>O as the sole byproduct.

---

## Introduction

Catalysis is a fact of our daily lives. A wide variety of important commercial chemical substances are currently produced on both the fine and bulk scales in the presence of molecular catalysts that have been optimized based on specific factors such as efficiency, toxicity, cost, or a combination thereof. Recent advancements in cheminformatics-based machine learning (ML) offer chemists a way to bypass traditional Edisonian empiricism and develop more efficient approaches to optimizing catalysts.<sup>1–4</sup> Several groups have reported successful demonstrations of ML-driven optimizations of homogeneous catalysts such as phosphoric acids<sup>5–8</sup> and Lewis-basic ligands for metal-based catalysts involving phosphines, *N*-heterocyclic carbenes, and nitrogen-based ligands.<sup>9–18</sup>

Recent progress in frustrated Lewis pairs (FLPs)<sup>19,20</sup> has expanded the practical and sustainable application of main-group catalysis, e.g., enabling the hydrogenation of unsaturated molecules without toxic/precious metals.<sup>21–26</sup> In this context, the main-group-catalyzed reductive alkylation of amines with carbonyl compounds and H<sub>2</sub> via the generation of FLP species has been widely accepted as a waste-minimizing process that generates valuable *N*-alkylated amines, whereby H<sub>2</sub>O is the only by-product.<sup>23,27–31</sup> Our group<sup>30</sup> and that of Soós<sup>28</sup> have independently shown that triarylboranes effectively catalyze the reductive alkylation of a variety of amines with aldehydes in the presence of H<sub>2</sub>. Moreover, we have demonstrated that an FLP

that consists of Soós' borane, i.e., B(2,6-Cl<sub>2</sub>-C<sub>6</sub>H<sub>3</sub>)(2,3,5,6-F<sub>4</sub>-C<sub>6</sub>H)<sub>2</sub> (**B**<sup>1a</sup>),<sup>27</sup> and tetrahydrofuran (THF) exhibits good functional-group tolerance for aniline derivatives including halogens, hydroxyl, and amide groups (Figure 1).<sup>30</sup> However, the direct reductive alkylation of amino acids with H<sub>2</sub> has remained challenging, and such reactions have proceeded in only low-to-moderate yields even under forcing conditions. In terms of toxicity, the solvent THF, which also acts here as a Lewis base to generate FLPs with boranes, should be replaced with a less hazardous chemical.<sup>32,33</sup> Given the central role of the reductive alkylation of amines using carbonyl compounds in the synthesis of e.g. pharmaceuticals, bio-active molecules, and agrochemicals,<sup>34–36</sup> the development of a straightforward and greener protocol for derivatizing amino acids and peptides would be worthwhile.

To this end, we envisioned an ML-assisted approach to identify a suitable triarylborane that is able to efficiently catalyze the reductive alkylation of amino acids and peptides with H<sub>2</sub> through the construction of an *in-silico* library that includes a variety of unprecedented triarylboranes. Moreover, through the construction of this *in-silico* library, we aimed to contribute to the structural diversification of triarylboranes beyond the archetypical B(C<sub>6</sub>F<sub>5</sub>)<sub>3</sub>,<sup>37–40</sup> which should expand the utility of this compound class in catalysis, materials science, and other areas. It should be noted that Dyson and Corminboeuf et al. have

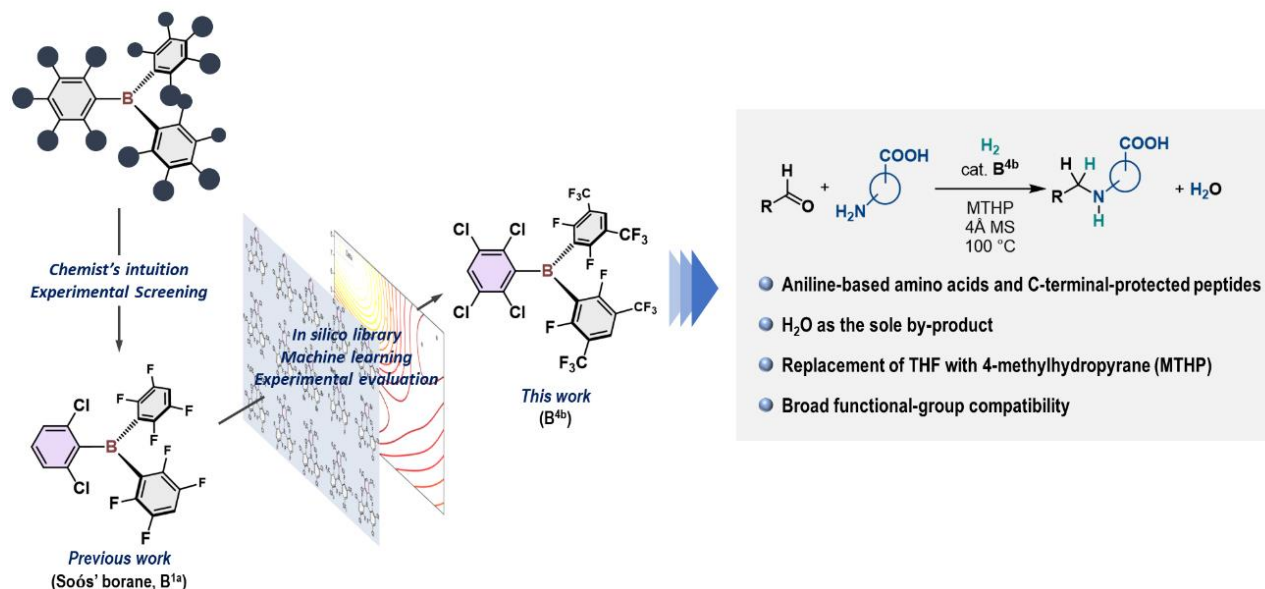


**Figure 1.** Schematic representation of the concept of this study.

recently demonstrated the hydrogenation of CO<sub>2</sub> to yield a formate salt [DBU–H][H–COO], which was catalyzed by an FLP consisting of tris(*p*-bromo)tridurylborane and 1,8-diazabicyclo[5.4.0]undec-7-ene (DBU). They identified this combination of borane and DBU using a cheminformatics-assisted approach that profiled the theoretically predicted catalyst activity based on the intrinsic acidity and basicity of the Lewis components.<sup>41</sup> Herein, we report the construction of an *in-silico* library with 54 triarylboranes, including 46 unprecedented structures, which was used for the ML-assisted identification of the optimal borane for the catalytic reductive alkylation of amino acids and peptides with aldehydes and H<sub>2</sub> (Figure 1). We also explored the functional-group compatibility of the present system using the functional group evaluation (FGE) kit recently proposed by Morimoto and Oshima et al.,<sup>42</sup> which is based on the concept of robustness screening that has been proposed by Glorius et al.<sup>43,44</sup>

## Results and discussion

We started our investigation with the construction of an *in-silico* library of triarylboranes using the strategy described below. Generally, we explored triarylboranes that seemed to be synthetically accessible using common procedures.<sup>37,40</sup> Optimization of the gas-phase structures of the 54 boranes shown in Figure 2A was accomplished using DFT calculations at the  $\omega$ B97X-D/6-311+G(d,p)// $\omega$ B97X-D/6-31G(d,p) level. The 53 explored heteroleptic boranes **B<sup>xy</sup>** ( $x = 1-6$ ,  $y = a-w$ ) include two 2,6-F<sub>2</sub>-3,5-R<sub>2</sub>-C<sub>6</sub>H groups, and their core structures are classified as **B<sup>1</sup>**–**B<sup>6</sup>** depending on the R groups, i.e., **B<sup>1</sup>**(F), **B<sup>2</sup>**(Cl), **B<sup>3</sup>**(Br), **B<sup>4</sup>**(CF<sub>3</sub>), and **B<sup>5</sup>**(H), whereas **B<sup>6</sup>** includes 2,6-F<sub>2</sub>-3-Cl-C<sub>6</sub>H<sub>2</sub> groups. With these core structures, we combined 23 aryl groups (**a**–**w**), and completed the construction of the borane library with the addition of B(C<sub>6</sub>F<sub>5</sub>)<sub>3</sub>. It should be noted that boranes **B<sup>xa</sup>** ( $x = 1-3$ , 5–6), **B<sup>1v</sup>**, and **B<sup>1w</sup>** were known before the construction of this library,<sup>27,30,45–47</sup> and their reactivity in the hydrogenation of unsaturated molecules inspired us when designing the library molecules. In fact, **B<sup>1a</sup>** has previously been employed for the catalytic reductive alkylation of aniline derivatives to generate active FLP species with THF,<sup>30</sup> and thus, *in-silico* derivatization of **B<sup>1a</sup>** was carried out via substitution of the *meta* and/or *para* H atoms in the 2,6-Cl<sub>2</sub>-C<sub>6</sub>H<sub>3</sub>

group with Cl, Br, CF<sub>3</sub>, OMe, OCF<sub>3</sub> or C<sub>6</sub>F<sub>5</sub> groups. We further conducted extensive *in-silico* derivatization of **B<sup>2a</sup>** and **B<sup>3a</sup>**, given that these boranes exhibit far superior catalytic activity than **B<sup>1a</sup>**, **B<sup>6a</sup>**, and B(C<sub>6</sub>F<sub>5</sub>)<sub>3</sub> in the hydrogenation of *N*-heteroaromatics using a gaseous mixture of H<sub>2</sub>/CO/CO<sub>2</sub>/CH<sub>4</sub>.<sup>45</sup> In these cases, we envisioned that the modulation of the intrinsic Lewis acidity of the triarylboranes, i.e., the energy levels of the LUMO, which includes the *p* orbital on the boron center,<sup>48</sup> as well as the remote back-strain<sup>49</sup> that influences the stability of the four-coordinated tetrahedral Lewis base–borane adducts. The introduction of 2,6-Br<sub>2</sub>-C<sub>6</sub>H<sub>3</sub> (**j**) and its derivatives (**k–r**) into the **B<sup>2</sup>** core was also explored, as we expected an increase in the front strain that influences the accessibility of the Lewis bases to the boron centers.<sup>37</sup>

We subsequently obtained the theoretical parameters. We thought that the use of structural parameters obtained from the gas-phase optimization of **B<sup>xy</sup>** would not play a critical role in predicting the reactivity of the triarylboranes under the chosen conditions, given that no substantial differences were observed among them (Table S3). Thus, we obtained the following energetic parameters: (i) the energy levels of the LUMOs [eV], which include the *p* orbitals on the boron atoms, (ii) the energy barriers ( $\Delta G_{H^\ddagger}$  in kcal mol<sup>–1</sup>) for the heterolytic cleavage of H<sub>2</sub> with the combination of **B<sup>xy</sup>** and THF, and (iii) the relative Gibbs energy values ( $\Delta G_{w^\circ}$ ) [kcal mol<sup>–1</sup>] for the formation of the H<sub>2</sub>O–**B<sup>xy</sup>** adducts with respect to [H<sub>2</sub>O + **B<sup>xy</sup>**]. These theoretical values are shown in Figure 3A for some selected boranes. For parameter (ii), we have previously proposed that the heterolytic cleavage of H<sub>2</sub> by FLPs should be involved in the rate-determining event of the **B<sup>1a</sup>**-catalyzed reductive alkylation of amines.<sup>30</sup> For parameter (iii), H<sub>2</sub>O could be a potential quencher of the triarylborane catalysts via the formation of adducts followed by proto-deboronation.<sup>50</sup> In this context, we envisioned that boranes **B<sup>xy</sup>** that exhibit larger  $\Delta G_{w^\circ}$  and smaller  $\Delta G_{H^\ddagger}$  values should show superior performance as Lewis acids for the generation of more active FLPs with ethereal components. It should also be mentioned here that we theoretically optimized a structure that included a sole imaginary frequency related to the H–H bond cleavage; however, to reduce the calculation costs, we performed an IRC calculation only for selected cases

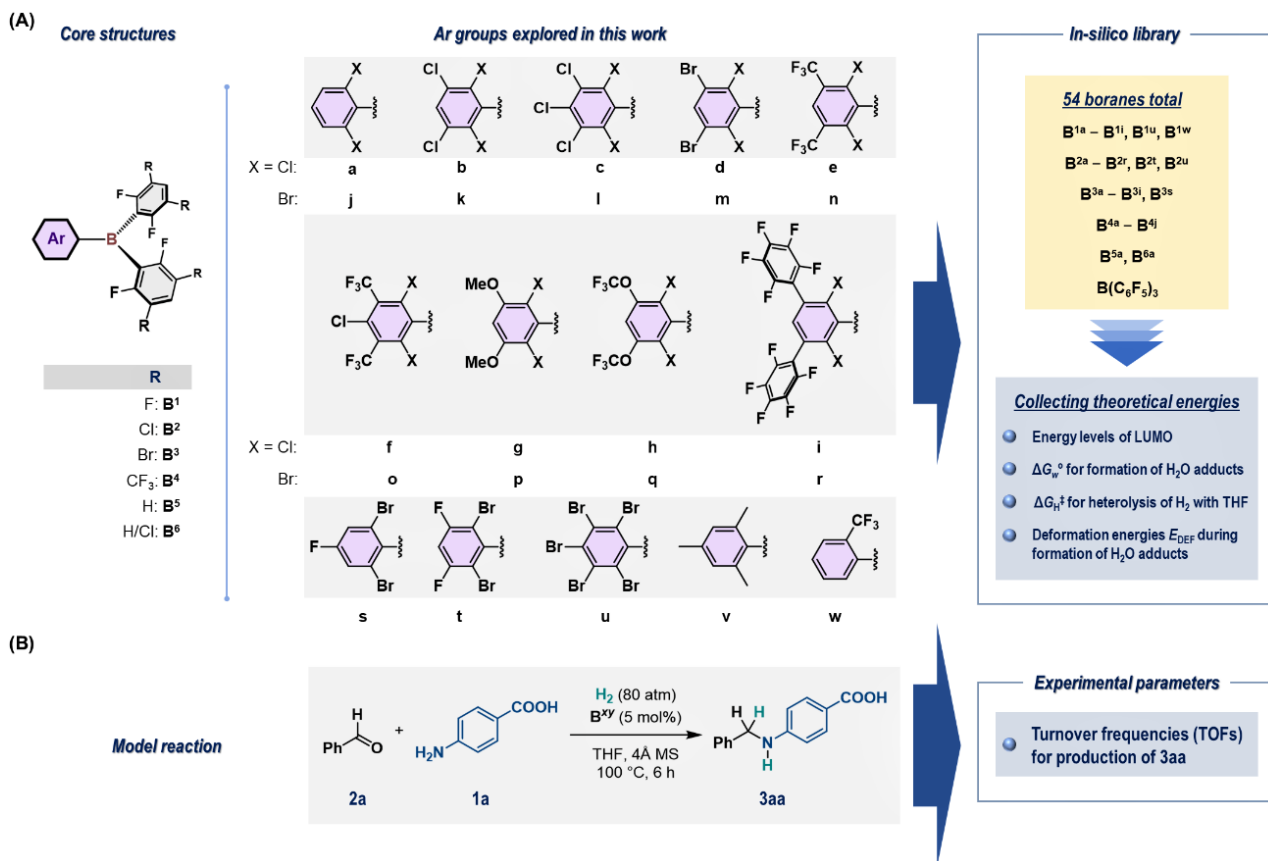


**Figure 2.** (A) The *in-silico* library of triarylboranes explored in this work. The structure of **B<sup>6</sup>** includes 2,6-F<sub>2</sub>-3-Cl-C<sub>6</sub>H<sub>2</sub> groups. (B) The model reaction for obtaining the experimental parameters (turnover frequencies per hour) used in this work.

and confirmed their validity as a possible transition state structure.

Next, we turned our attention to collecting experimental data for the reported triarylboranes (**B<sup>1a</sup>**,  $x = 1-3, 5, 6$ ; **B<sup>1v</sup>**; **B<sup>1w</sup>**;  $B(C_6F_5)_3$ ) and newly synthesized boranes (**B<sup>1f</sup>**; **B<sup>2y</sup>**,  $y = b, c, e$ ; **B<sup>3y</sup>**,  $y = b, c, s$ ); the latter compounds were used to analyze the influence of the derivatization of the 2,6-Cl<sub>2</sub>-C<sub>6</sub>H<sub>3</sub> structure. We obtained the turnover frequency (TOF in h<sup>-1</sup>; Figure 3A) as an experimental parameter calculated based on the yield of **3aa** from the reductive alkylation of amino acid **1a** with benzaldehyde (**2a**) and H<sub>2</sub> in the presence of 5 mol% **B<sup>xy</sup>** under the shown conditions as a model reaction (Figure 2B). The design of this model reaction is based on the potential of **B<sup>1a</sup>** to produce **3aa** in approximately 50% yield after 6 h (i.e., TOF = 1.67 h<sup>-1</sup>), as this consideration allows for a clearer evaluation of the positive and negative effects of structural derivatization during the optimization of **B<sup>xy</sup>**.

With the theoretical and experimental parameters in hand, Gaussian process regression (GPR), which is a radial basis function kernel-based statistical-learning algorithm, using GPy (a programming library for GPR),<sup>51</sup> was applied to construct a model to predict the TOF values for the production of **3aa** (it should be noted here that unless stated otherwise, mean values are presented for the theoretically predicted TOF values).<sup>52</sup> GPR using GPy constructs a regression model using a limited number of observed data through ML and searches for a subsequent adequate parameter value of **B<sup>xy</sup>** using the surrogate model. We evaluated the accuracy of each GPR model based on the coefficient of determination ( $Q^2$ ) of the leave-one-out (LOO) cross-validation using either training or validation data.

It is noteworthy that  $Q^2$  values range between 0 and 1, whereby higher values indicate a more robust explanation for the data. We carried out the initial GPR analysis using the experimental TOF values and pairs of two of the three theoretical parameters (LUMO energy level,  $\Delta G_w^\circ$ , and  $\Delta G_H^\ddagger$ ) obtained for the 15 boranes shown in Figure 3A as training data. This GPR analysis resulted in three distinct models, labelled **Model I** ( $\Delta G_w^\circ$  vs  $\Delta G_H^\ddagger$ ;  $Q^2 = 0.75$ ), **II** (LUMO level vs  $\Delta G_H^\ddagger$ ;  $Q^2 = 0.76$ ), and **III** (LUMO level vs  $\Delta G_w^\circ$ ;  $Q^2 = 0.18$ ) (Figure 3B). Subsequently, we used the theoretical parameters of the other 39 triarylboranes to predict their TOF values using these three models. We found intriguing inconsistencies among the TOF values for the **B<sup>4</sup>** derivatives that contain *meta*-CF<sub>3</sub> groups predicted using **Model I** and those predicted using **Model II** or **III** (Figure 3C). For example, when **Model I** was applied, the TOF values of **B<sup>4b</sup>**, **B<sup>4c</sup>**, and **B<sup>4e</sup>** were predicted to be 3.50, 3.66, and 3.59, respectively; however, using **Model II** (or **III**), the corresponding TOF values were predicted to be 0.55 (2.10), 0.23 (2.03), and 0.55 (1.92) respectively (Figures 3C and 3D). A critical difference between **Model I** and **Model II** or **III** is the use of the LUMO energy levels in the GPR analysis. Thus, to evaluate whether the LUMO levels can serve here as a critical parameter for the prediction of the TOF for the production of **3aa**, we additionally synthesized **B<sup>4b</sup>**, **B<sup>4c</sup>**, and **B<sup>4e</sup>**, and confirmed that these boranes demonstrate excellent activity for the reductive alkylation of **1a** with **2a** under the model reaction conditions (Figure 3D). Subsequently, we evaluated the root mean square errors (RMSE) of **Model I**, **II**, and **III** using the experimental TOF values for **B<sup>4b</sup>**, **B<sup>4c</sup>**, and **B<sup>4e</sup>** as test data; a model with a smaller RMSE value is considered more accurate. The accuracy of **Model I** (RMSE =

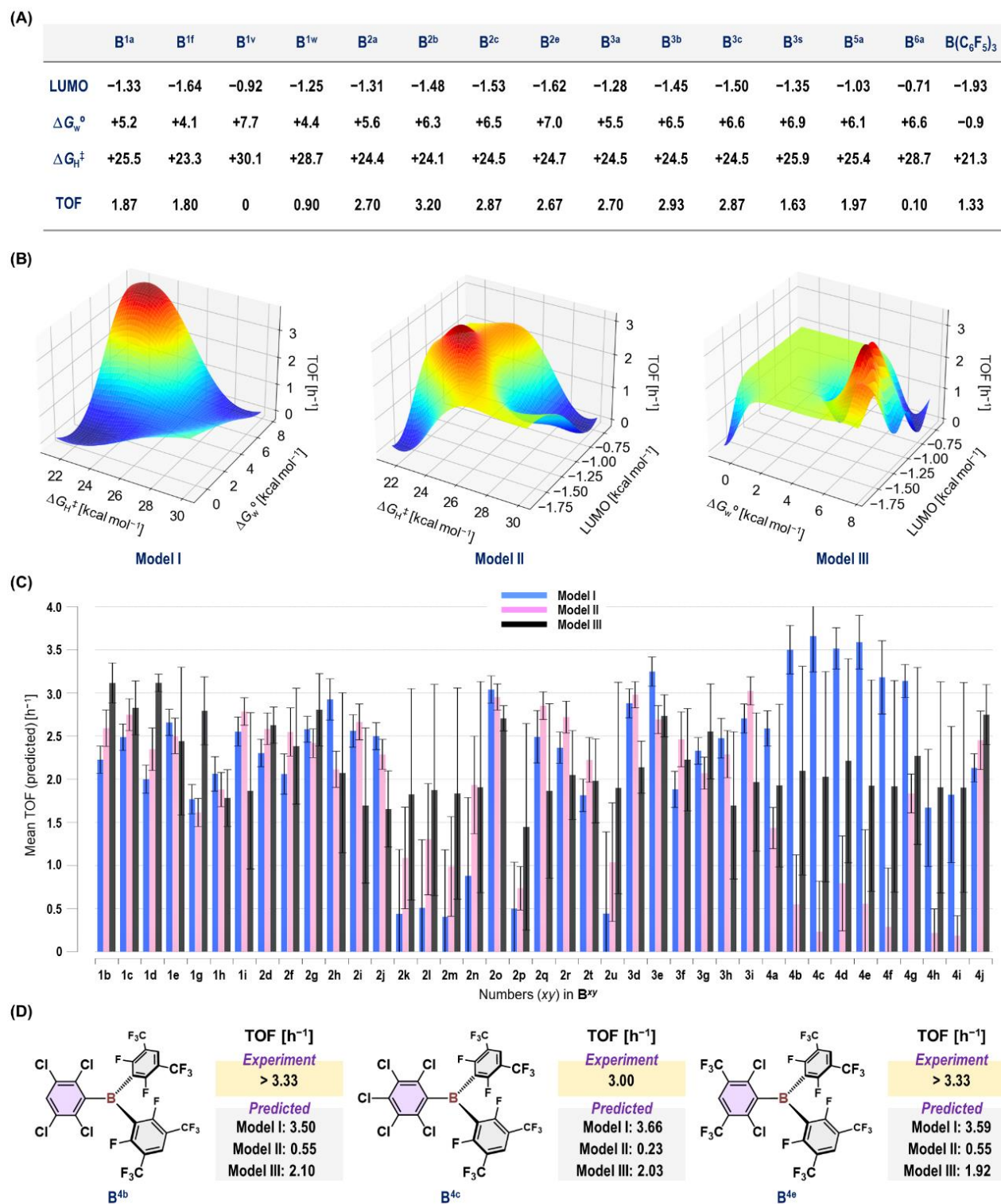


**Figure 3.** (A) LUMO energy level [eV],  $\Delta G_w^\circ$  [kcal mol<sup>-1</sup>], and  $\Delta G_H^\ddagger$  [kcal mol<sup>-1</sup>] for selected boranes **B<sup>xy</sup>**. TOFs [h<sup>-1</sup>] calculated based on the yield of **3aa** under the model conditions are also shown. (B) Gaussian process regression using the programming library GPy for the prediction of the TOF values. The theoretical values of the parameters  $\Delta G_w^\circ$  and  $\Delta G_H^\ddagger$  (**Model I**), the LUMO level and  $\Delta G_H^\ddagger$  (**Model II**), or the LUMO level and  $\Delta G_w^\circ$  (**Model III**) were used. (C) Comparison of the TOF values predicted using **Models I, II, or III**. Error bars represent 1 $\sigma$  standard deviation. (D) Comparison of the experimental and predicted TOF values for **B<sup>4b</sup>**, **B<sup>4c</sup>**, and **B<sup>4e</sup>**.

0.42 [h<sup>-1</sup>]) was confirmed to be greater than that of **Model II** (RMSE = 2.78 [h<sup>-1</sup>]) and **Model III** (RMSE = 1.22 [h<sup>-1</sup>])). These results indicate that **Model I** is the most adequate model for the prediction of the catalytic activity of **B<sup>xy</sup>** under the applied

conditions. Based on synthetic accessibility considerations, we finally decided to employ **B<sup>4b</sup>** as the optimal catalyst in the following experiments. These results also suggest that the employment of a theoretical parameter related to the intrinsic Lewis

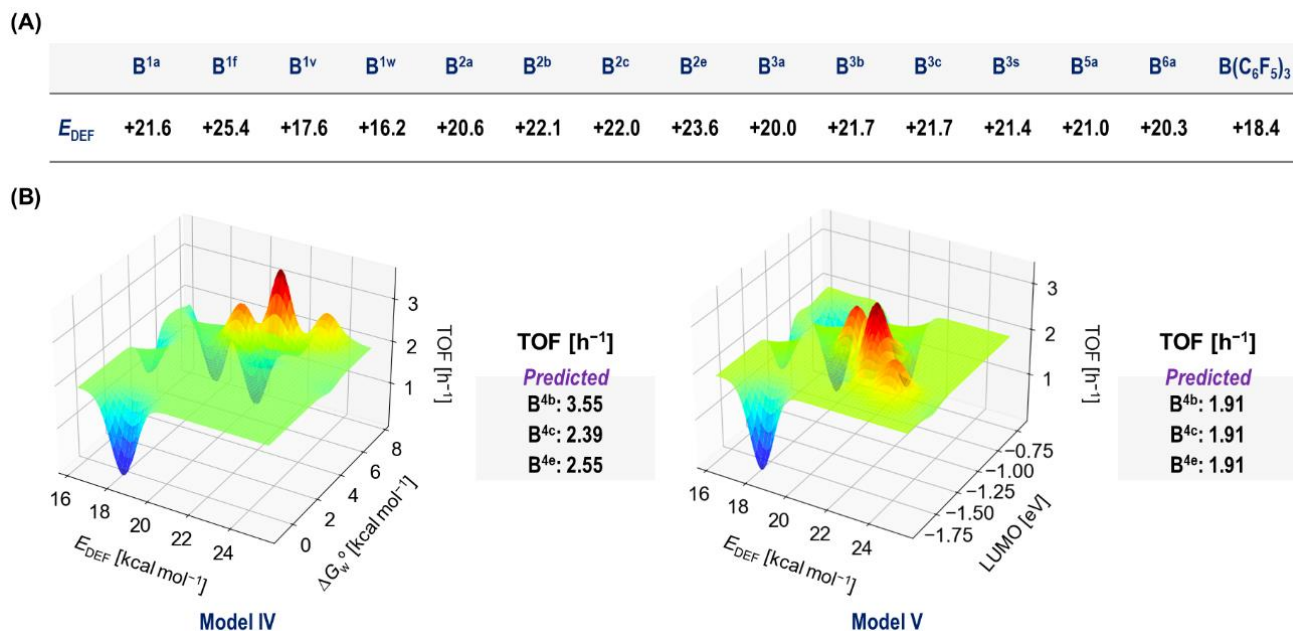


**Figure 4.** (A) Deformation energies ( $E_{\text{DEF}}$ ) [kcal mol<sup>-1</sup>] for selected boranes **B<sup>xy</sup>**. (B) Gaussian process regression with GPy for the prediction of TOF values [h<sup>-1</sup>], using either  $E_{\text{DEF}}$  and  $\Delta G_{\text{w}}^{\circ}$  (**Model IV**) or  $E_{\text{DEF}}$  and the LUMO level (**Model V**).

acidity of triarylboranes, such as the LUMO energy level, is inappropriate for the prediction of the catalytic activity of triarylboranes under the chosen conditions.

Although we successfully developed **Model I** for the prediction of the catalyst activity of **B<sup>xy</sup>**, the calculation of  $\Delta G_{\text{H}}^{\ddagger}$  via the DFT-based optimization of a possible transition state is relatively inefficient in terms of costs. We thus pursued the use of a different theoretical parameter for the construction of a regression-based model for the prediction of the TOF values. This parameter should be related to the steric properties of the *meta*-substituents with respect to the boron centers in **B<sup>xy</sup>**, given that the GPR analysis using the intrinsic electronic properties of the boranes failed to construct reliable prediction models (*vide supra*). In this context, we have recently proposed that the deformation energy ( $E_{\text{DEF}}$ ) [kcal mol<sup>-1</sup>] can be used to evaluate the degree of remote back-strain,<sup>49</sup> where  $E_{\text{DEF}}$  represents the energetic penalty associated with the change in the conformation at the boron center from trigonal planar to tetrahedral upon the formation of LB–borane adducts.<sup>48,53,54</sup> These results prompted us to examine whether the  $E_{\text{DEF}}$  value could serve as an adequate index for designing boranes **B<sup>xy</sup>** for the catalytic reductive alkylation of amino acids and peptides. We calculated the  $E_{\text{DEF}}$  values for the boranes shown in Figure 3A via the gas-phase optimization of their H<sub>2</sub>O adducts followed by energy-decomposition analysis at the RI-DSD-PBEP86-D3BJ/ma-Def2-QZVPP//PBEh-3c/Def2-SVP level (Figure 4A). The GPR analysis with  $E_{\text{DEF}}$  and  $\Delta G_{\text{w}}^{\circ}$  using the experimental TOF values shown in Figure 3A as training data resulted in the construction of **Model IV** ( $Q^2 = 0.20$ ), which exhibits nearly adequate predictions for the TOF values in the production of **3aa**, as exemplified by the cases with **B<sup>4b</sup>** (3.55), **B<sup>4c</sup>** (2.39), and **B<sup>4e</sup>** (2.55) (Figure 4B, left). In contrast, **Model V** ( $Q^2 = 0.13$ ), which was generated using the identical training data and the  $E_{\text{DEF}}$  and LUMO level, obviously underestimates the TOF values (1.91 in all cases), similar to the predictions of **Model III** (Figure 4B, right). Identical conclusions were confirmed when comparing the RMSE values of **Model IV** (0.59) and **V** (1.33) using the

experimental TOF values for **B<sup>4b</sup>**, **B<sup>4c</sup>**, and **B<sup>4e</sup>** as test data. These results indicate that the  $E_{\text{DEF}}$  can be a useful indicator to predict the activity of triarylboranes, at least under the present reaction conditions. Moreover, **Model V** again demonstrates that the inclusion of LUMO levels leads to underestimation of the TOF values.

With the optimal triarylborane **B<sup>4b</sup>** in hand, we modified the reaction conditions to reduce its environmental impact and thus establish a greener and more sustainable system. In this context, the use of an alternative reaction solvent that could also act as a Lewis base to generate an FLP with **B<sup>4b</sup>** was initially explored, given the recent demand for the replacement of hazardous THF with alternative ethereal compounds that exhibit lower toxicity combined with high chemical and thermal stability.<sup>32</sup> In the presence of 40 atm H<sub>2</sub>, the reductive alkylation of **1a** with **2a** was carried out using THF, 2-methyltetrahydrofuran (2-MeTHF), cyclopentyl methyl ether (CPME), 4-methyltetrahydropyran (MTHP), or 2,2,4-trimethyl-1,3-dioxolane (TMD) (Figure 5A). While THF provided a superior result (50%) compared to 2-MeTHF (38%) and CPME (18%), **3aa** was generated in 59% yield when MTHP was used. Prolongation of the reaction time to 24 h resulted in the formation of **3aa** in 72% yield; however, the removal of the 4 Å MS caused a significant decrease in the yield of **3aa** to 42%. Finally, increasing the H<sub>2</sub> pressure to 60 atm resulted in the formation of **3aa** in 95% yield. The use of TMD did not furnish any **3aa**. It should be noted that MTHP can be easily separated from water (its solubility in H<sub>2</sub>O is ~1.5 wt%) and removed under reduced pressure due to its strong hydrophobicity and low heat of vaporization, although its employment as a greener solvent has been limited in organic synthesis compared with the use of 2-MeTHF and CPME.<sup>32,33</sup> Moreover, to clarify the benefit of using MTHP over THF, we compared the activation energies for the heterolytic cleavage of H<sub>2</sub> by the combination of **B<sup>4b</sup>** and THF or MTHP at the  $\omega$ B97X-D/6-311+G(d,p)// $\omega$ B97X-D/6-31G(d,p) level (Figure 5B). A possible transition state was found in both cases, and that in the case of MTHP was found to be more stabilized ( $\text{TS}_{\text{MTHP}} = +21.8$

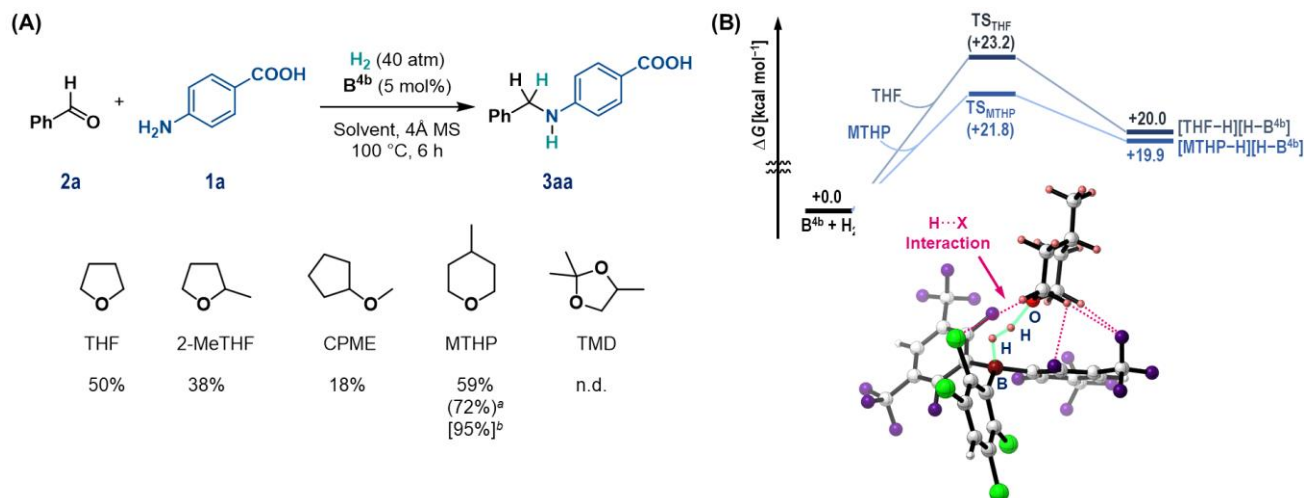


**Figure 5.** (A) Exploration of greener Lewis-basic solvents. Reaction conditions: **1a** (0.4 mmol, 0.05 M), **2a** (1.0 equiv.), **B<sup>4b</sup>** (5 mol%), and 4Å MS (100 mg) were mixed in the solvent, followed by pressurization with H<sub>2</sub> (40 atm). The yield of **3aa** was determined via <sup>1</sup>H NMR analysis. <sup>a</sup>24 h. <sup>b</sup>60 atm H<sub>2</sub>. (B) Relative Gibbs free energies [kcal mol<sup>-1</sup>] with respect to [B<sup>4b</sup> + H<sub>2</sub> + LB], where LB is either MTHP or THF, calculated at the ωB97X-D/6-311+G(d,p)//ωB97X-D/6-31G(d,p) level. The structure of TS<sub>MTHP</sub> is also shown. Pairs of atoms involved in H...X (F/Cl) interactions that were found using AIM analysis are indicated by dashed lines (H: pink; B: brown; C: gray; O: red; F: purple; Cl: light green).

kcal mol<sup>-1</sup>) than that in the case involving THF (TS<sub>THF</sub> = +23.2 kcal mol<sup>-1</sup>). We attribute this stabilization to the increased structural flexibility of the tetrahydropyran motif relative to THF, which allows the formation of efficient non-covalent interactions (NCIs) between the F/Cl atoms in B<sup>4b</sup> and the H atoms in MTHP. The participation of such NCIs was confirmed using the quantum theory of atoms in molecules (AIM) method (for details, see Figure S13).<sup>55,56</sup>

The B<sup>4b</sup>-catalyzed reductive alkylation of **1a** with **2a** in MTHP using H<sub>2</sub> (40 atm) demonstrated remarkable compatibility toward a variety of additives (**A0–A21**) (Figure 6). All these experiments were carried out twice, and mean values [%] are given for the yield of **3aa**, the recovered additive, and the imine intermediate 4-(benzylideneamino)benzoic acid formed *in situ* through the B<sup>4b</sup>-catalyzed condensation of **1a** and **2a**. Initially, we carried out a control experiment using **A0**, which confirmed that the yields of **3aa** and the remaining imine were consistent (72% and 28%, respectively) with those of the reaction conducted without **A0** (Figures 5A and 6). Relative to the control experiment, the reductive alkylation among **1a**, **2a**, and H<sub>2</sub> proceeded without a significant change in the yield of **3aa**, the recovered additives, or imine intermediates for additives with ketone (**A3/A13**), primary amide (**A4**), aryl bromide/iodide including alkyl ether (**A6/A7**), allylic ether (**A8**), terminal alkyne (**A9**), enone (**A12**), nitrile (**A15**), and ester (**A20**) moieties. It is also noteworthy that additives including sulfhydryl (**A16**) and sulfide (**A17**) moieties did not affect the present reaction, whereas such sulfur-containing compounds can be critical inhibitors in transition-metal-based catalysis and organocatalysis.<sup>42</sup> On the other hand, the hydrogenation of the imine intermediates was obviously suppressed in the presence of aliphatic/aromatic carboxy (**A1/A14**), aliphatic hydroxyl (**A2**), bulky silyl ether (**A10**), pinacolboronyl (**A18**), and *N*-tert-butoxycarbonyl (Boc) (**A21**) moieties, as these functional groups include either a Lewis-basic or -acidic site that can kinetically inhibit the formation of the FLP consisting of B<sup>4b</sup> and MTHP. In fact, the quantitative recovery of the additives after a period of 24 h was confirmed, without the generation of any

other significant byproduct, i.e., the sum of the yields of **3aa** and the imine was always ~95%). In contrast, the formation of **3aa** was largely suppressed under reaction conditions including *N*-heteroaromatic moieties such as an imidazole (**A5**) and an indole (**A19**), as these heteroaromatic units can react with B<sup>4b</sup> to form classical Lewis adducts and/or aldehydes to complicate the system. In the case of **A11**, which includes an epoxide moiety, **3aa** was only produced in 13% yield, and a significant loss of **A11** was confirmed after the reaction. Given that Lewis-acidic triarylboranes mediate the ring-opening transformation of epoxides,<sup>57,58</sup> the B<sup>4b</sup>-catalyzed ring-opening reaction of **A11** to give the corresponding aldehyde can be expected to compete with the targeted reaction (see Supporting Information for details).

Finally, we applied the combination of B<sup>4b</sup> and MTHP for the reductive alkylation of amino acids and peptide derivatives in the presence of H<sub>2</sub> (Figure 7). Aminosalicyclic acids **1b** and **1c** were effectively alkylated under the optimized conditions, and **3ba** and **3ca** were obtained in 90% and 93% yield, respectively; 60 atm of H<sub>2</sub> was used in the latter case. For comparison, under a pressure of 80 atm of H<sub>2</sub> in THF, **3ba** and **3ca** were furnished in 47% and 70% yield in the presence of 10 mol% and 15 mol% B<sup>1a</sup>, respectively, which again demonstrates the advantages of the present system using B<sup>4b</sup> and MTHP in terms of synthetic efficiency and sustainability. The reductive alkylation of anthranilic acid (**1d**), which is also known as vitamin L1, 5-aminoisophthalic acid (**1e**), and 4-aminophenylacetic acid (**1f**) afforded **3da**, **3ea**, and **3fa** in excellent yield using 40–60 atm of H<sub>2</sub>. In contrast, we recognized that aliphatic amino acids (or their imine derivatives) and substrates insoluble in MTHP were not suitable. For example, aspartic acid (**1g**) is insoluble in MTHP, and no reaction took place when **1g** was employed under otherwise identical conditions. Esterification of the carboxy group in 3-amino-4,4-dimethylpentanoic acid effectively improved its solubility in MTHP. Moreover, the hydrogenation of the imine derived from **1h** and **2a** did not occur. Based on these results, we prepared alanine- and *S*-methylcysteine-based

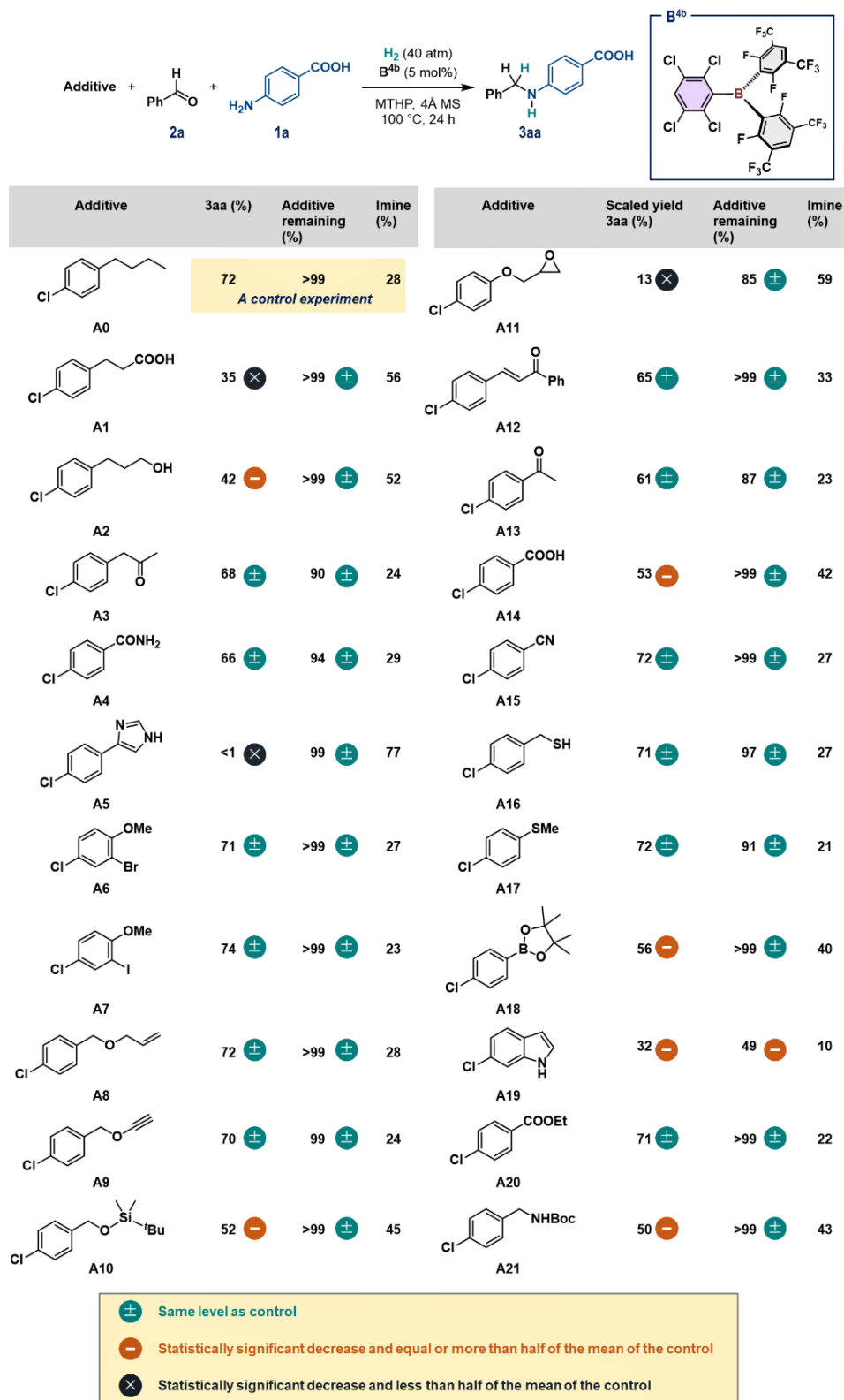


**Figure 6.** Exploring functional-group compatibility. Reaction conditions: **1a** (0.4 mmol, 0.05 M), **2a** (1.0 equiv.), additive (1.0 equiv.), **B<sup>4b</sup>** (5 mol%) and 4Å MS (100 mg) were mixed in MTHHP, followed by pressurization with H<sub>2</sub> (40 atm). The mean values of two experiments are given, which were determined via <sup>1</sup>H NMR analysis.

peptides **1i** and **1j**, and subjected them to the optimal reaction conditions; alkylated peptides **3ia** and **3ja** were obtained in 95% and 55% yield, respectively. In terms of the scope of aldehydes, 3,5-bis(trifluoromethyl)benzaldehyde (**2b**) furnished **3ab** in

93% yield, but 3,5-di-*tert*-butylbenzaldehyde (**2c**) gave **3ca** in merely 38%. In the latter case, a significant amount of **2c** remained unreacted, indicating difficulties associated with the formation of the imine intermediate due to the decreased

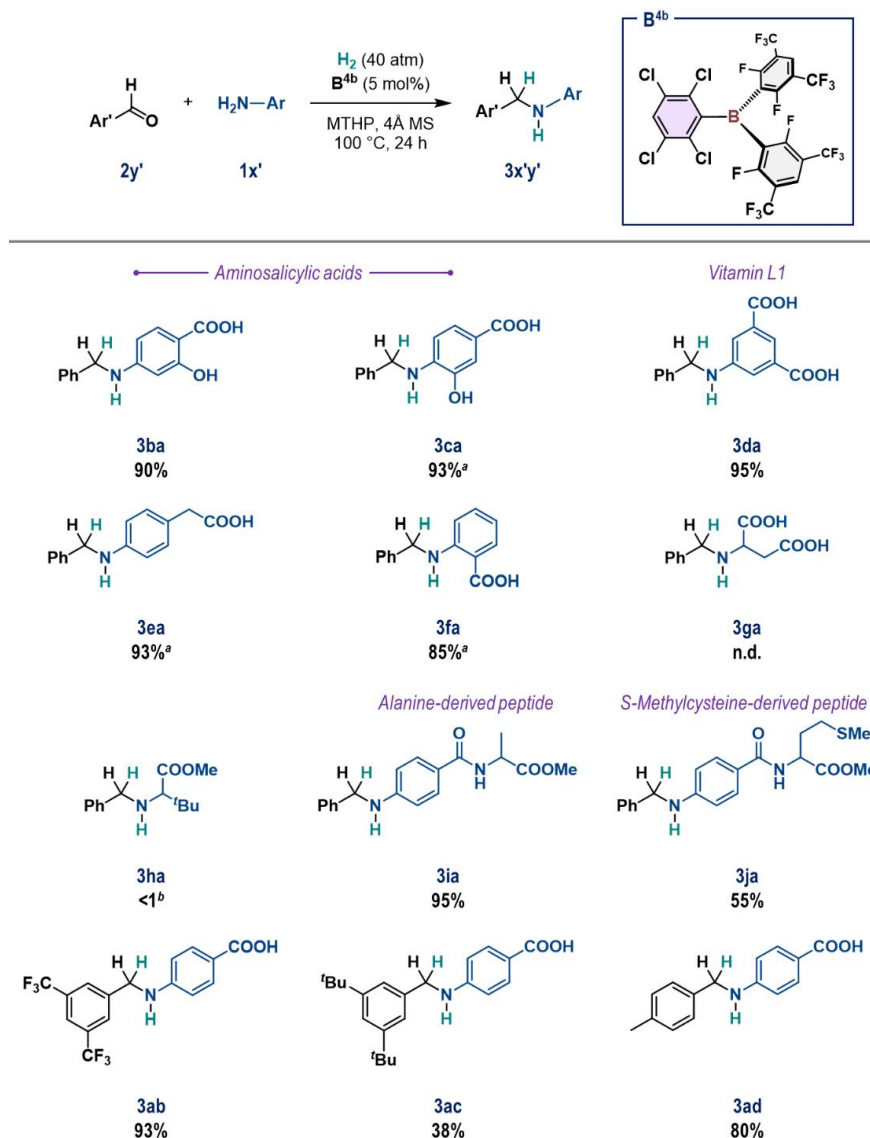


**Figure 7.** The  $\text{B}^{4b}$ -catalyzed reductive alkylation of amino acids (**1a–1h**) and peptides (**1i** and **1j**) with aldehydes (**2a–d**) using  $\text{H}_2$  in MTHP. General conditions: **1** (0.4 mmol, 0.05 M), **2** (1.0 equiv.),  $\text{B}^{4b}$  (5 mol%), and 4Å MS (100 mg) were mixed in MTHP, followed by pressurization with  $\text{H}_2$  (40 atm). Yields of isolated products are given. <sup>a</sup>60 atm  $\text{H}_2$ . <sup>b</sup>The formation of the imine in >99% was confirmed.

electrophilicity of the aldehyde moiety. A comparable result was obtained when *p*-tolualdehyde (**2d**) was used with respect to the case using **2a**, and **3da** was afforded in 80% yield.

### Conclusion

The present study demonstrates an *in-silico*-assisted approach to design triarylboranes that exhibit promising reactivity as main-group catalysts for the reductive alkylation of amino acids with  $\text{H}_2$ . We constructed an *in-silico* library of triarylboranes, including 46 unprecedented boranes, and obtained their theoretical parameters using DFT calculations. We initially synthesized seven of these unprecedented boranes to confirm their reactivity under the chosen model reaction conditions. Guided by Gaussian process regression using these theoretical and experimental parameters, we subsequently synthesized three more boranes and identified the optimal triarylborane, i.e., B(2,3,5,6-Cl<sub>4</sub>-C<sub>6</sub>H)(2,6-F<sub>2</sub>-3,5-(CF<sub>3</sub>)<sub>2</sub>-C<sub>6</sub>H)<sub>2</sub> ( $\text{B}^{4b}$ ). Through the evaluation of the regression-based models, we confirmed that the deformation energy ( $E_{\text{DEF}}$ ) may serve as a potentially useful

parameter to construct an adequate model, while the use of LUMO energy levels tends to lead to an underestimation when predicting the catalyst activity (TOF in  $\text{h}^{-1}$ ) under the model reaction conditions. We also identified that 4-methyltetrahydropyran (MTHP) is a superior Lewis-basic solvent for not only the generation of FLP species with  $\text{B}^{4b}$ , but also for the realization of a more practical and sustainable reaction system compared to a system using THF. In fact, the  $\text{B}^{4b}$ -catalyzed reductive alkylation using aldehydes as an alkylating reagent and  $\text{H}_2$  in MTHP proceeded efficiently even in the presence of a variety of additives, showcasing its broad functional-group compatibility. Aniline-derived amino acids and C-terminal-protected peptides were alkylated in good-to-excellent yields under the optimized conditions with the concomitant generation of  $\text{H}_2\text{O}$  as the sole byproduct, demonstrating the significant advancement in terms of practicality and sustainability for the main-group-catalyzed reductive functionalization of valuable amines using  $\text{H}_2$ .



## ASSOCIATED CONTENT

This material is available free of charge via the Internet at <http://pubs.acs.org>.

## AUTHOR INFORMATION

### Corresponding Author

\*hoshimoto@chem.eng.osaka-u.ac.jp

### Notes

The authors declare no competing financial interest.

## ACKNOWLEDGMENT

We thank Kuraray Co., Ltd., for providing 4-methyltetrahydropyrene. This project was supported by Grants-in-Aid for Transformative Research Area (A) Digitalization-Driven Transformative Organic Synthesis (JSPS KAKENHI grants 22H05363 to Y.Ho. and 21H05217 to S.T.) as well as the Environment Research and Technology Development Fund (JPMEERF20211R01 to Y.Ho.) of the Environmental Restoration and Conservation Agency of the Ministry of the Environment of Japan. Part of this work was supported by JST SPRING (grant JPMJSP2138 to Y.Hi.). Parts of the calculations were performed using resources from the Research Center for Computational Science, Okazaki, Japan (22-IMS-C107 and 23-IMS-C094).

## REFERENCES

- (1) Vogiatzis, K. D.; Polynski, M. V.; Kirkland, J. K.; Townsend, J.; Hashemi, A.; Liu, C.; Pidko, E. A. Computational Approach to Molecular Catalysis by 3d Transition Metals: Challenges and Opportunities. *Chem. Rev.* **2019**, *119*, 2453–2523.
- (2) Toyao, T.; Maeno, Z.; Takakusagi, S.; Kamachi, T.; Takigawa, I.; Shimizu, K. Machine Learning for Catalysis Informatics: Recent Applications and Prospects. *ACS Catal.* **2020**, *10*, 2260–2297.
- (3) Foscatto, M.; Jensen, V. R. Automated in Silico Design of Homogeneous Catalysts. *ACS Catal.* **2020**, *10*, 2354–2377.
- (4) Matsubara, S. Digitization of Organic Synthesis — How Synthetic Organic Chemists Use AI Technology —. *Chem. Lett.* **2021**, *50*, 475–481.
- (5) Zahrt, A. F.; Athavale, S. V.; Denmark, S. E. Quantitative Structure–Selectivity Relationships in Enantioselective Catalysis: Past, Present, and Future. *Chem. Rev.* **2020**, *120*, 1620–1689.
- (6) Rinehart, N. I.; Zahrt, A. F.; Henle, J. J.; Denmark, S. E. Dreams, False Starts, Dead Ends, and Redemption: A Chronicle of the Evolution of a Chemoinformatic Workflow for the Optimization of Enantioselective Catalysts. *Acc. Chem. Res.* **2021**, *54*, 2041–2054.
- (7) Crawford, J. M.; Kingston, C.; Toste, F. D.; Sigman, M. S. Data Science Meets Physical Organic Chemistry. *Acc. Chem. Res.* **2021**, *54*, 3136–3148.
- (8) Liles, J. P.; Rouget-Virbel, C.; Wahlman, J. L. H.; Rahimoff, R.; Crawford, J. M.; Medlin, A.; O'Connor, V. S.; Li, J.; Roytman, V. A.; Toste, F. D.; Sigman, M. S. Data Science Enables the Development of a New Class of Chiral Phosphoric Acid Catalysts. *Chem* **2023**, *9*, 1518–1537.
- (9) Chen, H.; Yamaguchi, S.; Morita, Y.; Nakao, H.; Zhai, X.; Shimizu, Y.; Mitsunuma, H.; Kanai, M. Data-Driven Catalyst Optimization for Stereodivergent Asymmetric Synthesis by Iridium/Boron Hybrid Catalysis. *Cell Rep. Phys. Sci.* **2021**, *2*, 100679.
- (10) Gensch, T.; Dos Passos Gomes, G.; Friederich, P.; Peters, E.; Gaudin, T.; Pollice, R.; Jorner, K.; Nigam, A.; Lindner-D'Addario, M.; Sigman, M. S.; Aspuru-Guzik, A. A Comprehensive Discovery Platform for Organophosphorus Ligands for Catalysis. *J. Am. Chem. Soc.* **2022**, *144*, 1205–1217.
- (11) Xu, J.; Grosslight, S.; Mack, K. A.; Nguyen, S. C.; Clagg, K.; Lim, N.-K.; Timmerman, J. C.; Shen, J.; White, N. A.; Sirois, L. E.; Han, C.; Zhang, H.; Sigman, M. S.; Gosselin, F. Atroposelective Negishi Coupling Optimization Guided by Multivariate Linear Regression Analysis: Asymmetric Synthesis of KRAS G12C Covalent Inhibitor GDC-6036. *J. Am. Chem. Soc.* **2022**, *144*, 20955–20963.
- (12) Karl, T. M.; Bouayad-Gervais, S.; Hueffel, J. A.; Sperger, T.; Wellig, S.; Kaldas, S. J.; Dabranskaya, U.; Ward, J. S.; Rissanen, K.; Tizzard, G. J.; Schoenebeck, F. Machine Learning-Guided Development of Trialkylphosphine Ni<sup>(0)</sup> Dimers and Applications in Site-Selective Catalysis. *J. Am. Chem. Soc.* **2023**, *145*, 15414–15424.
- (13) Goebel, J. F.; Löffler, J.; Zeng, Z.; Handelsmann, J.; Hermann, A.; Rodstein, I.; Gensch, T.; Gessner, V. H.; Gooßen, L. J. Computer-Driven Development of Ylide Functionalized Phosphines for Palladium-Catalyzed Hiyama Couplings. *Angew. Chem., Int. Ed.* **2023**, *62*, e202216160.
- (14) Huang, H.; Zong, H.; Bian, G.; Yue, H.; Song, L. Correlating the Effects of the N-Substituent Sizes of Chiral 1,2-Amino Phosphinamide Ligands on Enantioselectivities in Catalytic Asymmetric Henry Reaction Using Physical Steric Parameters. *J. Org. Chem.* **2014**, *79*, 9455–9464.
- (15) See, X. Y.; Wen, X.; Wheeler, T. A.; Klein, C. K.; Goodpaster, J. D.; Reiner, B. R.; Tonks, I. A. Iterative Supervised Principal Component Analysis Driven Ligand Design for Regioselective Ti-Catalyzed Pyrrole Synthesis. *ACS Catal.* **2020**, *10*, 13504–13517.
- (16) Mukai, M.; Nagao, K.; Yamaguchi, S.; Ohmiya, H. Molecular Field Analysis Using Computational-Screening Data in Asymmetric N-Heterocyclic Carbene-Copper Catalysis toward Data-Driven *In Silico* Catalyst Optimization. *Bull. Chem. Soc. Jpn.* **2022**, *95*, 271–277.
- (17) Wang, J.-W.; Li, Z.; Liu, D.; Zhang, J.-Y.; Lu, X.; Fu, Y. Nickel-Catalyzed Remote Asymmetric Hydroalkylation of Alkenyl Ethers to Access Ethers of Chiral Dialkyl Carbinols. *J. Am. Chem. Soc.* **2023**, *145*, 10411–10421.
- (18) Cordova, M.; Wodrich, M. D.; Meyer, B.; Sawatlon, B.; Corninboeuf, C. Data-Driven Advancement of Homogeneous Nickel Catalyst Activity for Aryl Ether Cleavage. *ACS Catal.* **2020**, *10*, 7021–7031.
- (19) Stephan, D. W.; Erker, G. Frustrated Lewis Pair Chemistry: Development and Perspectives. *Angew. Chem., Int. Ed.* **2015**, *54*, 6400–6441.
- (20) Jupp, A. R.; Stephan, D. W. New Directions for Frustrated Lewis Pair Chemistry. *Trends Chem.* **2019**, *1*, 35–48.
- (21) Weicker, S. A.; Stephan, D. W. Main Group Lewis Acids in Frustrated Lewis Pair Chemistry: Beyond Electrophilic Boranes. *Bull. Chem. Soc. Jpn.* **2015**, *88*, 1003–1016.
- (22) Scott, D. J.; Fuchter, M. J.; Ashley, A. E. Designing Effective 'Frustrated Lewis Pair' Hydrogenation Catalysts. *Chem. Soc. Rev.* **2017**, *46*, 5689–5700.
- (23) Hoshimoto, Y.; Ogoshi, S. Triarylborane-Catalyzed Reductive N-Alkylation of Amines: A Perspective. *ACS Catal.* **2019**, *9*, 5439–5444.
- (24) Fasano, V.; Ingleson, M. Recent Advances in Water-Tolerance in Frustrated Lewis Pair Chemistry. *Synthesis* **2018**, *50*, 1783–1795.
- (25) Paradies, J. Structure–Reactivity Relationships in Borane-Based FLP-Catalyzed Hydrogenations, Dehydrogenations, and Cycloisomerizations. *Acc. Chem. Res.* **2023**, *56*, 821–834.
- (26) Feng, X.; Du, H. Metal-Free Asymmetric Hydrogenation and Hydrosilylation Catalyzed by Frustrated Lewis Pairs. *Tetrahedron Lett.* **2014**, *55*, 6959–6964.
- (27) Gyömöre, Á.; Bakos, M.; Földes, T.; Pápai, I.; Domján, A.; Soós, T. Moisture-Tolerant Frustrated Lewis Pair Catalyst for Hydrogenation of Aldehydes and Ketones. *ACS Catal.* **2015**, *5*, 5366–5372.
- (28) Dorkó, É.; Szabó, M.; Kótai, B.; Pápai, I.; Domján, A.; Soós, T. Expanding the Boundaries of Water-Tolerant Frustrated Lewis Pair Hydrogenation: Enhanced Back Strain in the Lewis Acid Enables the Reductive Amination of Carbonyls. *Angew. Chem., Int. Ed.* **2017**, *56*, 9512–9516.
- (29) Sapsford, J. S.; Scott, D. J.; Allcock, N. J.; Fuchter, M. J.; Tighe, C. J.; Ashley, A. E. Direct Reductive Amination of Carbonyl Compounds Catalyzed by a Moisture Tolerant Tin(IV) Lewis Acid. *Adv. Synth. Catal.* **2018**, *360*, 1066–1071.
- (30) Hoshimoto, Y.; Kinoshita, T.; Hazra, S.; Ohashi, M.; Ogoshi, S. Main-Group-Catalyzed Reductive Alkylation of Multiply Substituted Amines with Aldehydes Using H<sub>2</sub>. *J. Am. Chem. Soc.* **2018**, *140*, 7292–7300.
- (31) Zhao, J.; Liu, S.; Liu, S.; Ding, W.; Liu, S.; Chen, Y.; Du, P. A Theoretical Study on the Borane-Catalyzed Reductive Amination of Aniline and Benzaldehyde with Dihydrogen: The Origins of Chemoselectivity. *J. Org. Chem.* **2022**, *87*, 1194–1207.
- (32) Bijoy, R.; Agarwala, P.; Roy, L.; Thorat, B. N. Unconventional

- Ethereal Solvents in Organic Chemistry: A Perspective on Applications of 2-Methyltetrahydrofuran, Cyclopentyl Methyl Ether, and 4-Methyltetrahydropyran. *Org. Process Res. Dev.* **2022**, *26*, 480–492.
- (33) Samoïlov, V.; Ni, D.; Goncharova, A.; Zarezin, D.; Kniazeva, M.; Ladesov, A.; Kosyakov, D.; Bermeshev, M.; Maximov, A. Bio-Based Solvents and Gasoline Components from Renewable 2,3-Butanediol and 1,2-Propanediol: Synthesis and Characterization. *Molecules* **2020**, *25*, 1723.
- (34) Bryan, M. C.; Dunn, P. J.; Entwistle, D.; Gallou, F.; Koenig, S. G.; Hayler, J. D.; Hickey, M. R.; Hughes, S.; Kopach, M. E.; Moine, G.; Richardson, P.; Roschangar, F.; Steven, A.; Weiberth, F. J. Key Green Chemistry Research Areas from a Pharmaceutical Manufacturers' Perspective Revisited. *Green Chem.* **2018**, *20*, 5082–5103.
- (35) Murugesan, K.; Senthamarai, T.; Chandrashekar, V. G.; Natte, K.; Kamer, P. C. J.; Beller, M.; Jagadeesh, R. V. Catalytic Reductive Aminations Using Molecular Hydrogen for Synthesis of Different Kinds of Amines. *Chem. Soc. Rev.* **2020**, *49*, 6273–6328.
- (36) Roughley, S. D.; Jordan, A. M. The Medicinal Chemist's Toolbox: An Analysis of Reactions Used in the Pursuit of Drug Candidates. *J. Med. Chem.* **2011**, *54*, 3451–3479.
- (37) Carden, J. L.; Dasgupta, A.; Melen, R. L. Halogenated Triarylboranes: Synthesis, Properties and Applications in Catalysis. *Chem. Soc. Rev.* **2020**, *49*, 1706–1725.
- (38) He, J.; Rauch, F.; Finze, M.; Marder, T. B. (Hetero)Arene-Fused Boroles: A Broad Spectrum of Applications. *Chem. Sci.* **2021**, *12*, 128–147.
- (39) Kumar, G.; Roy, S.; Chatterjee, I. Tris(Pentafluorophenyl)Borane Catalyzed C–C and C–Heteroatom Bond Formation. *Org. Biomol. Chem.* **2021**, *19*, 1230–1267.
- (40) Berger, S. M.; Ferger, M.; Marder, T. B. Synthetic Approaches to Triarylboranes from 1885 to 2020. *Chem. - Eur. J.* **2021**, *27*, 7043–7058.
- (41) Das, S.; Turnell-Ritson, R. C.; Dyson, P. J.; Corminboeuf, C. Design of Frustrated Lewis Pair Catalysts for Direct Hydrogenation of CO<sub>2</sub>. *Angew. Chem., Int. Ed.* **2022**, *61*, e202208987.
- (42) Saito, N.; Nawachi, A.; Kondo, Y.; Choi, J.; Morimoto, H.; Ohshima, T. Functional Group Evaluation Kit for Digitalization of Information on the Functional Group Compatibility and Chemoselectivity of Organic Reactions. *Bull. Chem. Soc. Jpn.* **2023**, *96*, 465–474.
- (43) Collins, K. D.; Glorius, F. A Robustness Screen for the Rapid Assessment of Chemical Reactions. *Nat. Chem.* **2013**, *5*, 597–601.
- (44) Collins, K. D.; Glorius, F. Intermolecular Reaction Screening as a Tool for Reaction Evaluation. *Acc. Chem. Res.* **2015**, *48*, 619–627.
- (45) Hashimoto, T.; Asada, T.; Ogoshi, S.; Hoshimoto, Y. Main Group Catalysis for H<sub>2</sub> Purification Based on Liquid Organic Hydrogen Carriers. *Sci. Adv.* **2022**, *8*, eade0189.
- (46) Erős, G.; Nagy, K.; Mehdi, H.; Pápai, I.; Nagy, P.; Király, P.; Tárkányi, G.; Soós, T. Catalytic Hydrogenation with Frustrated Lewis Pairs: Selectivity Achieved by Size-Exclusion Design of Lewis Acids. *Chem. - Eur. J.* **2012**, *18*, 574–585.
- (47) Dorkó, É.; Kótai, B.; Földes, T.; Gyömöre, Á.; Pápai, I.; Soós, T. Correlating Electronic and Catalytic Properties of Frustrated Lewis Pairs for Imine Hydrogenation. *J. Organomet. Chem.* **2017**, *847*, 258–262.
- (48) Erdmann, P.; Greb, L. What Distinguishes the Strength and the Effect of a Lewis Acid: Analysis of the Gutmann–Beckett Method. *Angew. Chem., Int. Ed.* **2022**, *61*, e202114550.
- (49) Sakuraba, M.; Morishita, T.; Hashimoto, T.; Ogoshi, S.; Hoshimoto, Y. Remote Back Strain: A Strategy for Modulating the Reactivity of Triarylboranes. *Synlett* **2023**, a-2110-5359.
- (50) Fasano, V.; Radcliffe, J. E.; Ingleson, M. J. B(C<sub>6</sub>F<sub>5</sub>)<sub>3</sub>-Catalyzed Reductive Amination Using Hydrosilanes. *ACS Catal.* **2016**, *6*, 1793–1798.
- (51) The GPy authors. GPy: A Gaussian process framework in python. <http://github.com/SheffieldML/Gpy>
- (52) Kondo, M.; Wathsala, H. D. P.; Sako, M.; Hanatani, Y.; Ishikawa, K.; Hara, S.; Takaai, T.; Washio, T.; Takizawa, S.; Sasai, H. Exploration of Flow Reaction Conditions Using Machine-Learning for Enantioselective Organocatalyzed Rauhut–Currier and [3+2] Annulation Sequence. *Chem. Commun.* **2020**, *56*, 1259–1262.
- (53) Rodrigues Silva, D.; De Azevedo Santos, L.; Freitas, M. P.; Guerra, C. F.; Hamlin, T. A. Nature and Strength of Lewis Acid/Base Interaction in Boron and Nitrogen Trihalides. *Chem. - Asian J.* **2020**, *15*, 4043–4054.
- (54) Timoshkin, A. Y.; Davydova, E. I.; Sevastianova, T. N.; Suvorov, A. V.; Schaefer, H. F. Relationship between the Energy of Donor–Acceptor Bond and the Reorganization Energy in Molecular Complexes. *Int. J. Quantum Chem.* **2002**, *88*, 436–440.
- (55) Kumar, P. S. V.; Raghavendra, V.; Subramanian, V. Bader's Theory of Atoms in Molecules (AIM) and Its Applications to Chemical Bonding. *J. Chem. Sci.* **2016**, *128*, 1527–1536.
- (56) Macchi, P. Chemical Bonding in Transition Metal Carbonyl Clusters: Complementary Analysis of Theoretical and Experimental Electron Densities. *Coord. Chem. Rev.* **2003**, *238–239*, 383–412.
- (57) Bhagat, M. N.; Bennett, C. K.; Chang, G.-F.; Zhu, Y.; Raghuraman, A.; Belowich, M. E.; Nguyen, S. T.; Broadbelt, L. J.; Notestein, J. M. Enhancing the Regioselectivity of B(C<sub>6</sub>F<sub>5</sub>)<sub>3</sub>-Catalyzed Epoxide Alcoholysis Reactions Using Hydrogen-Bond Acceptors. *ACS Catal.* **2019**, *9*, 9663–9670.
- (58) Andrea, K. A.; Kerton, F. M. Triarylborane-Catalyzed Formation of Cyclic Organic Carbonates and Polycarbonates. *ACS Catal.* **2019**, *9*, 1799–1809.

